

Modelling and Analysis of a Power Transformer Using Finite Element Analysis

Sabo Sani Muhammad¹, Sabo Abdulrazak², G. A. Bakare³,
Sabo Abdulhafiz⁴, D. M. Nazif⁵

^{1,2,3}Abubakar Tafawa Balewa University Bauchi, Nigeria; ⁴Sa'adu Zungur University, Bauchi,
Nigeria; ⁵Federal Polytechnic Bauchi, Nigeria
saborinji@gmail.com

Article Info:

Submitted:	Revised:	Accepted:	Published:
Apr 8, 2025	Apr 28, 2025	May 13, 2025	May 18, 2025

Abstract

This study presents an enhanced Finite Element Method (FEM) model for comprehensive analysis of power transformers, addressing electromagnetic, thermal, and electrostatic performance aspects with improved accuracy and efficiency. Conventional analytical approaches to evaluating transformer characteristics—such as core losses, copper losses, magnetic flux distribution, and thermal behavior—are often labor-intensive and susceptible to inaccuracies. To overcome these limitations, a double discretization FEM (DD-FEM) framework was developed using ANSYS Maxwell and ANSYS Mechanical software to simulate a 30 MVA, 132/33 kV three-phase power transformer. The electromagnetic simulation yielded core and copper losses of 19.62 kW and 97.03 kW, respectively, with DD-FEM reducing absolute errors by 1.38% and 1.48% compared to standard FEM methods. Thermal modeling under normal loading conditions indicated a peak winding temperature of 94.2°C, rising to 112.9°C during overloading (33 MVA), thus justifying the need for forced cooling systems. Electrostatic analysis confirmed that electric

field stresses between windings remained within safe operational limits (10.48 kV/mm²), though a localized insulation weakness was identified between the low-voltage winding and the core (3.74 kV/mm²). Across all evaluated parameters, the DD-FEM model showed superior alignment with benchmark analytical results, reducing relative errors in core loss estimation by up to 12.2%. These results affirm the efficacy of the enhanced FEM approach in optimizing transformer design, enhancing operational reliability, and reducing engineering uncertainty, particularly under varying load and fault scenarios. The study demonstrates the critical role of advanced numerical tools in modern transformer engineering and high-fidelity system simulation.

Keywords: Finite Element Method; Power transformer; Electromagnetic analysis; Thermal modeling; ANSYS Maxwell; Transformer losses.

INTRODUCTION

Engineers worldwide face challenges in modeling power transformers, a costly component in energy transmission networks. High-accuracy designs using Finite Element Analysis (FEA) and Finite Element Method (FEM) are essential for predicting parameters like electromagnetic forces, flux distribution, losses, and thermal distribution.

The study analyzes the efficiency of protective and shunt applications, electrical field distributions, insulation levels, magnetic field models, Laplace forces, and short circuit testing in transformer design. It also explores methods to reduce eddy current loss using FEM and double discretization or double meshing models.

The study employed computer simulations for transformer design, utilizing FEM for optimization and efficiency. A three-dimensional magnetostatic problem was solved using a finite element mesh. A combined electromechanical finite element method calculated inductance, core and winding losses, and transient voltage-current relations. This method provided a rough estimate of transformer characteristics and an analytical evaluation of parameter interval settings.

In this research, an enhanced model was developed for studying both the electromagnetic flux distribution and the loss of the transformer with thermal field analysis. Electromagnetic forces, electromagnetic flux, electric stresses, losses, and thermal distributions of transformers were investigated. The numerical results were compared with the analytical results.

The evaluation of power transformer performance characteristics, including temperature distribution, flux distribution, and losses, is a complex issue in electrical engineering. Nivashini (2020) developed the Finite Element Method for complex engineering analyses, including electromagnetic, magnetostatics, thermal conduction, structural mechanics, transients, fluid dynamics, and acoustics. This research presents an enhanced finite element model application for power transformers, focusing on electromagnetic, thermal, insulation, and winding model computation.

METHODS

Materials

The material used in the work includes the Personal Computer, Name Plate Rating of the Transformer (Table 1), Ansys Maxwell electronics, Ansys Mechanical, and Ansys Workbench. The electrical information used in the analysis of the transformer is presented in Table 1.

Table 1: Name plate rating of the proposed transformer

Quantity	Value
Power, MVA	30
Primary Voltage, kV	132
Secondary Voltage, kV	33
Circumscribing circle diameter (d), mm	701.23
Frequency, Hz	50
Height of window (H_w), mm	2125.7
Width of window (W_w), mm	1062.8
Connection Type	Ynd11
Connection	Star/Delta
Level of maximum turn	1476/1384
Primary Resistance (r_p), Ω	8.4299
Secondary Resistance (r_s), Ω	1.1703
Iron losses, kW	22.01
Ohmic losses, kW	104.22
PU Impedance	0.0634

The properties of the materials used to perform design and thermal analysis in the ANSYS@Maxwell environment are given in Table 2.

Table 2 Properties of the materials used

	Density(kg/m ³)	Conductivity(W/m ²⁰ C)
Core	7650	5
Winding	8933	400
Insulation material		4.5

Development of electromagnetic model of transformer

The study used ANSYS MAXWELL software to analyze transformer models using the finite element method. It estimated core losses, stray losses, DC losses, and winding eddy current losses. The program created windings, cores, terminals, and tanks, with geometrical and electrical values adjustable on the interface. The step-by-step method for achieving the development of the electromagnetic model is given in the flow diagram in Figure 1.

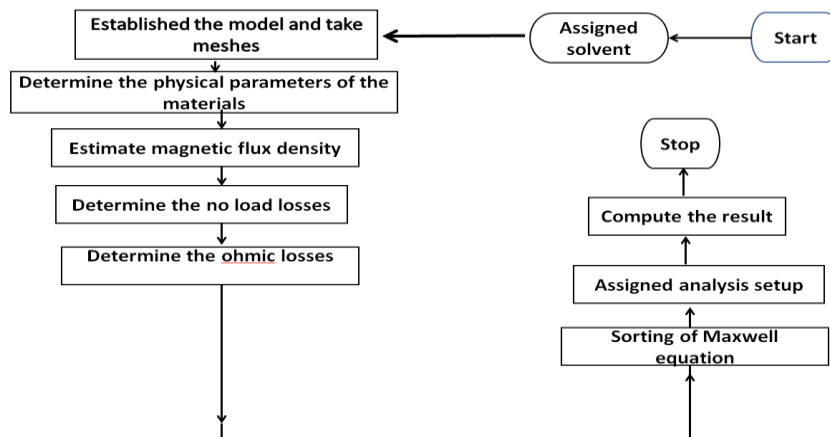


Figure 1: Flow chart of electromagnetic model

Mesh settings of the model

The ANSYS MAXWELL program generates a network automatically for model analysis, but this is insufficient for realistic results. To analyze real values, each element is divided into small regions, and the correct solution is achieved by increasing the mesh number.

Measurement of losses

The load loss and no-load loss experiments according to standard IEC 60076-7 were performed to obtain the copper loss and iron loss under rated conditions. A schematic diagram of the load loss test and no-load test is presented in Plates 1 and 2. The loss tests are performed at rated frequency (50Hz).

Short circuit test

The load loss is measured using voltage applied to high-voltage windings, revealing a low iron loss due to the high-voltage winding's low supply current.

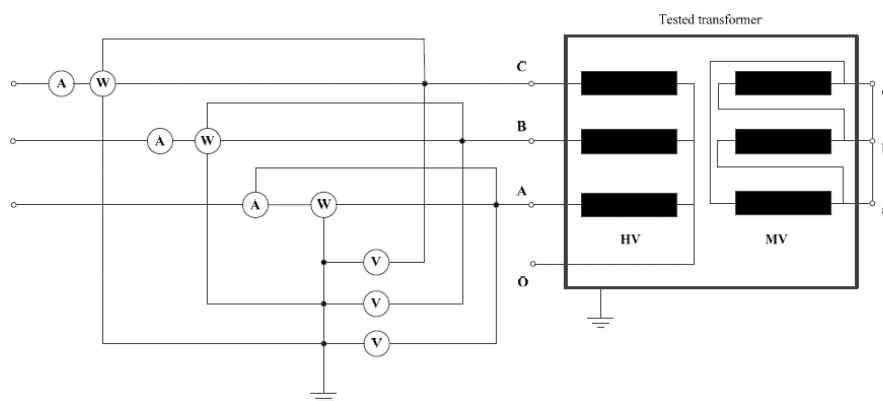


Plate 1: Load Test

Open circuit test

The transformer's core loss is measured using an open-circuit test, where the low-voltage winding is loaded at rated voltage and the high-voltage terminal is open-circuited.

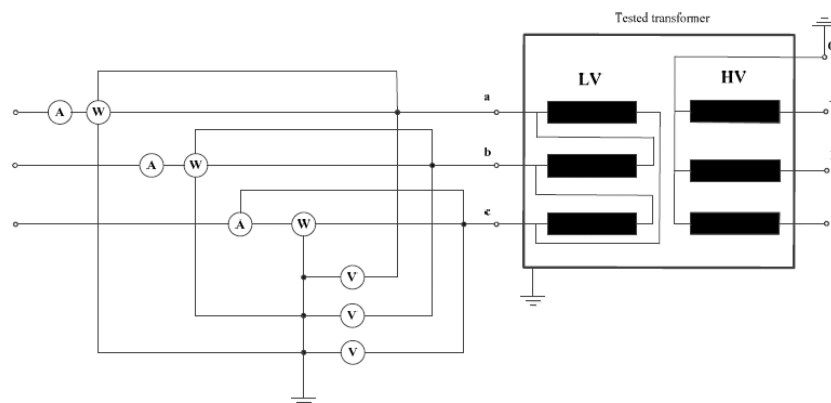


Plate 2: No Load Test

Electrodynamics force (winding) model of transformer

Following standard procedures, the effect of applying an external short circuit was represented by an injection of 2,783.52A at the HV and 11,134.04A at the LV windings.

The step-by-step method for achieving the development of the electrodynamic force model is given in the flow chart in Figure 2.

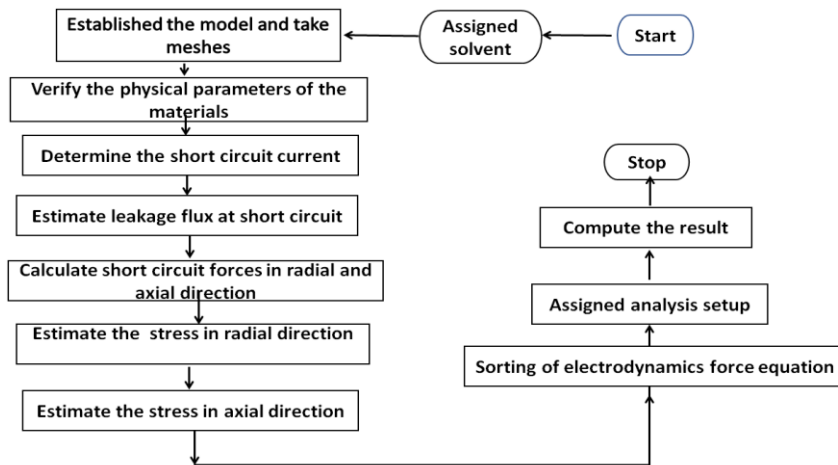


Figure 2: Flow chart of Electrodynamic analysis

Thermal model of transformer

In Figure 2 above, the model of the transformer designed in the ANSYS@Maxwell3D environment was presented. The flowchart of 3D coupled thermal analysis is shown in Figure 3.

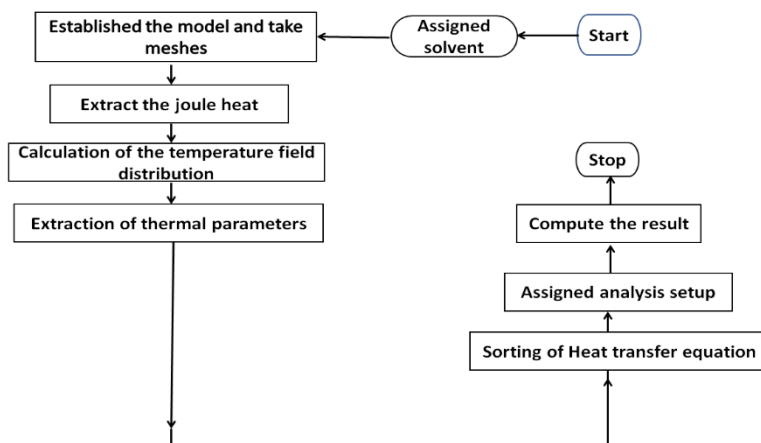


Figure 3: Flowchart of coupled thermal field analysis

Electrostatic analysis of the insulation model

Following standard procedures, the effect of applying an input voltage was represented by putting a voltage of 132000V at the HV and 33000V at the LV windings. The step-by-step method for achieving the development of the electrostatic model is given in the flow chart in Figure 4.

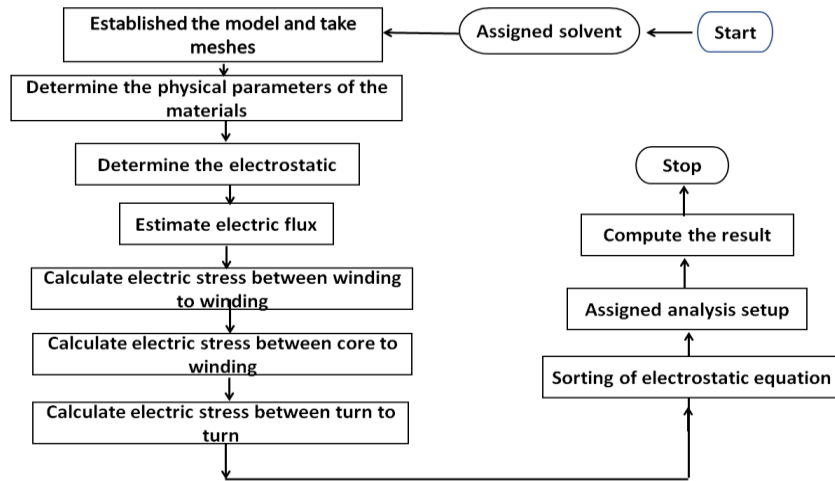


Figure 4: Flowchart of electrostatic analysis

RESULTS AND DISCUSSION

Electromagnetic Analysis Results

Individual output phases are shown along with their respective input voltages in Figure 5 seen that the output is a balanced three-phase supply from a three-phase input.

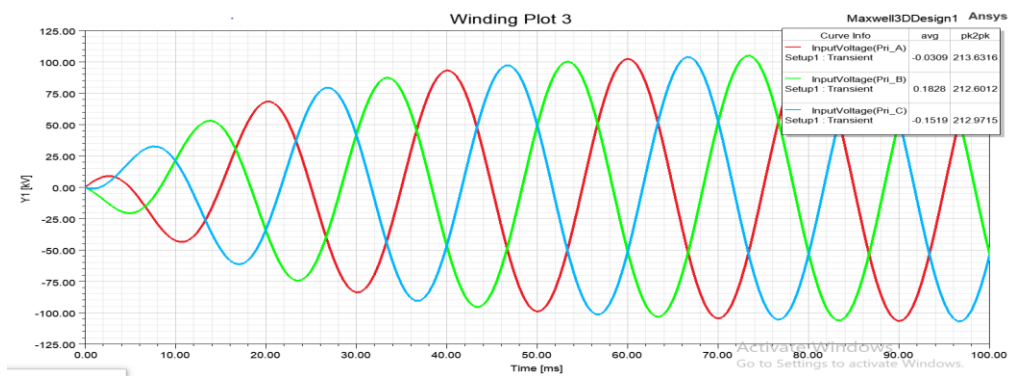


Figure 5: Input Primary Voltage of the transformer.

A slow rise, start-up exponential function was used to remove the inrush shown in Figure 5. The inrush phenomenon normally causes malfunctioning of the differential relay

at start-up energization. Hence, a slow rise start-up is introduced. Also, the differences in values of the input voltages, 213.63, 212.60, and 212.97 kV, are a result of the differences in the length of the limbs of the core.

Figure 6 represent the output voltage waveforms of the transformer from FEM.

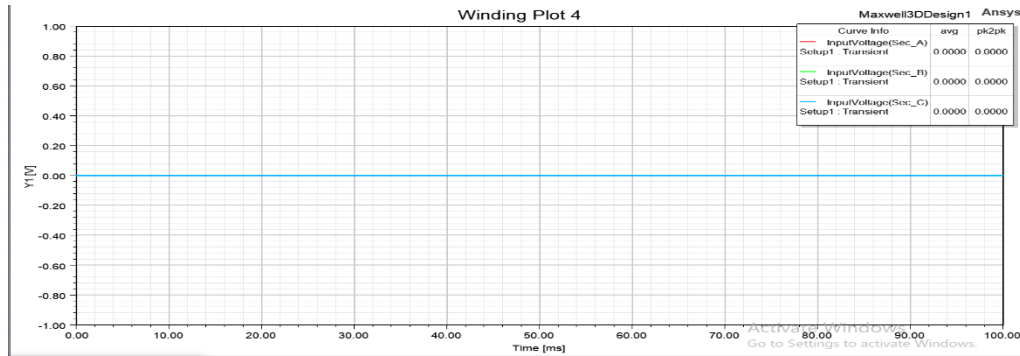


Figure 6: Secondary Voltage of the transformer.

Since the output is open-circuited, there wouldn't be any indication of voltage, which reads 0.00V for the three phases as shown in Figure 6.

Figure 7 provides the magnetizing current waveforms of the primary winding.

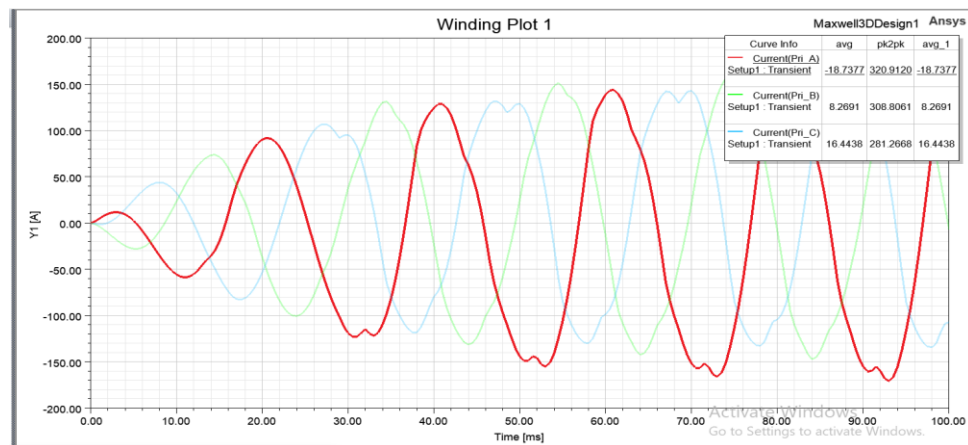


Figure 7: Magnetizing current of the transformer.

The average value obtained from the ANSYS MAXWELL simulation along the third limbs was 8.26A, with some spikes due to magnetization in the steel core materials.

Figure 8 shows the induced voltage of the primary and secondary windings.

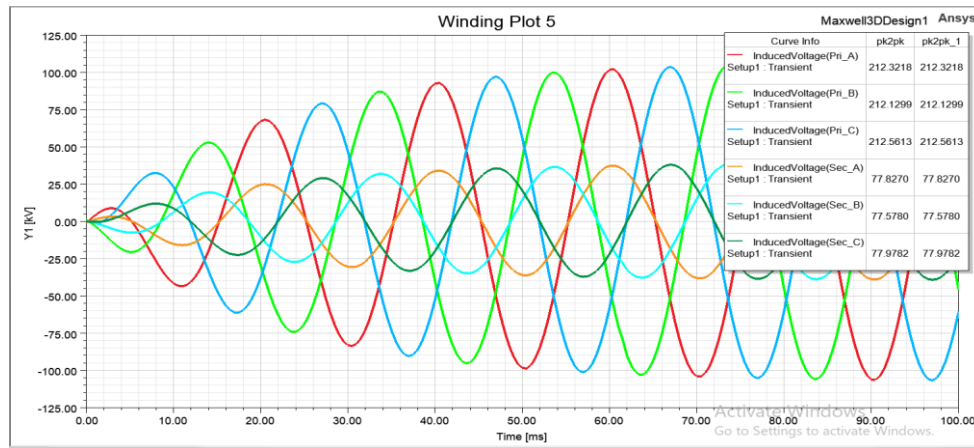


Figure 8: Superimposed Induced Primary and Secondary voltage of the transformer

It is observed that there is a perfect transformation of voltages at the core of the transformer due to the lesser difference between the induced and the input voltage as a result of the Faraday law of magnetism.

Figure 9 gives the flux linkage of the primary and secondary winding along the transformer core.

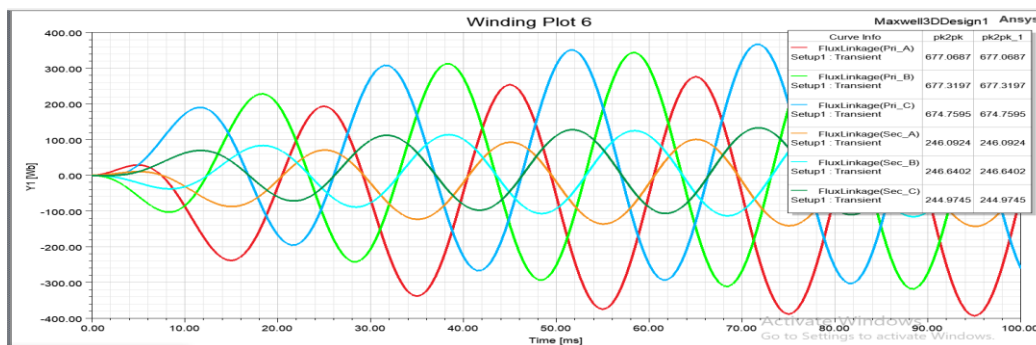


Figure 9: Superimposed Primary and Secondary flux linkage of the transformer

Satisfy that principle of analogy, where current is equivalent to flux. The primary and secondary input current is approximately equal to the flux linkage linking the primary and secondary of the transformer, with a value of 677.32 webers on limb B in the primary winding and 248.64 webers on the same limb in the secondary winding.

Figure 10 shows the secondary current of the no-load transformer in ANSYS MAXWELL.

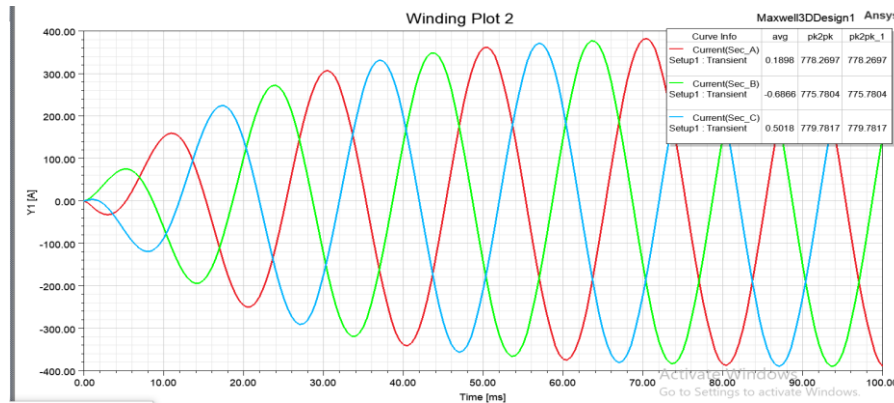


Figure 10: Induced Secondary current of the transformer

The secondary current value of the proposed transformer is given in Figure 10. It was noticed that a value of 775.78A along limb B is in close agreement with the analytical inputted values.

Figure 11 shows the plot of core loss v/s time.

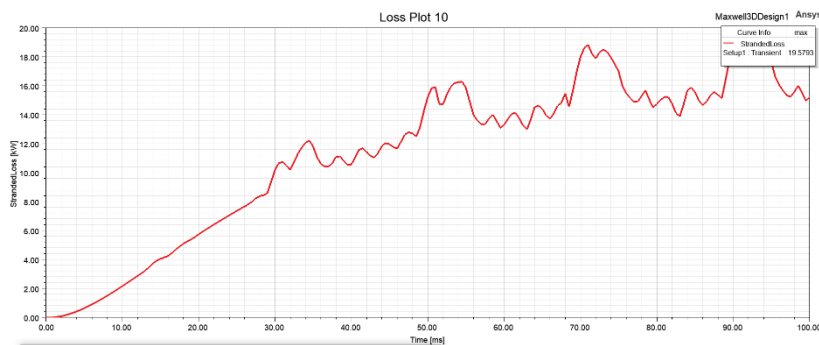


Figure 11: Core loss of the transformer

Core loss is the no-load loss, which does not change with the load. It can be seen that the core loss becomes stable within five cycles (as transient analysis was performed). The obtained value of core loss is 19.58 kW.

Figures 12 show the magnetic field distribution as well as the power transformer.

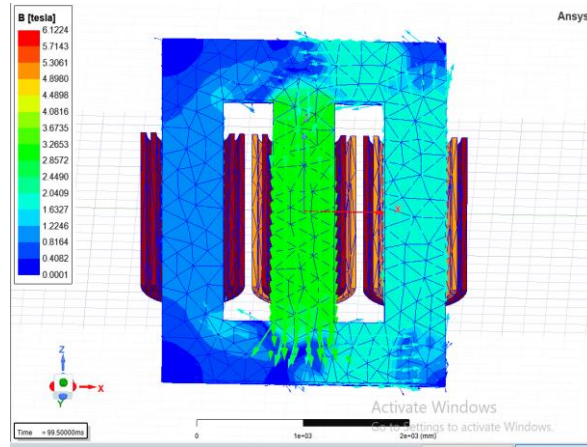


Figure 12: Magnetic flux distributions

It can be seen that when the red phase was excited alone, flux density was created in the limb of the Red phase, which doubled the flux density in the other two limbs, as shown in Figure 12. But, when red and blue phases were excited, the flux density created in the blue limb is the summation of what is at the yellow and red phases. From the nano plot, a minimum of 0.4082T and a maximum of 1.6232T, for 132 kV, were obtained.

Figure 13 provides the contour plot of the magnetic field strength.

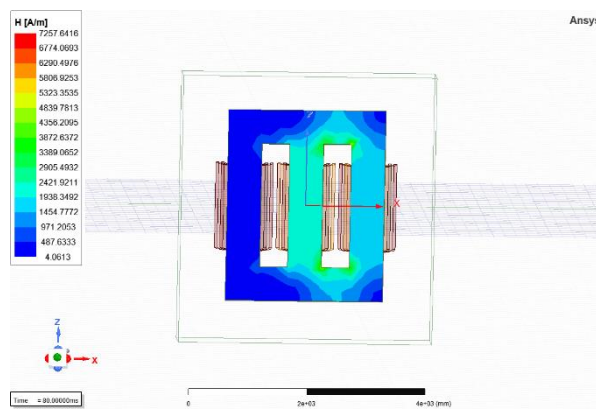


Figure 13: Magnetic field strength distribution

The direction of the flux lines is indicated in the magnetic field strength plot of Figure 13, showing how they were turning at an angle from the limbs towards the yokes, leading to higher losses in those areas. Difficulties must have occurred in the winding insulation, especially in those areas.

The contour plot current density of the proposed transformer is shown in Figure 14.

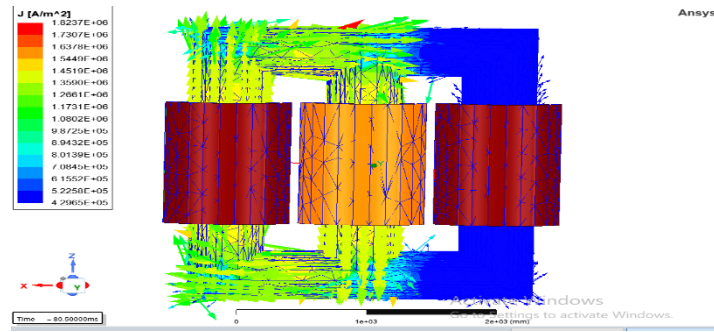


Figure 14: Current density distributions

It was observed that during the electromagnetic analysis, the current density obtained from a half 3D model of the transformer winding with a value of $1.26\text{A}/\text{mm}^2$ is in close agreement with an assumed current density of $2.3\text{A}/\text{mm}^2$ for a full 3D model.

Figure 15 shows the contour plot of the copper loss of the proposed 3D model.

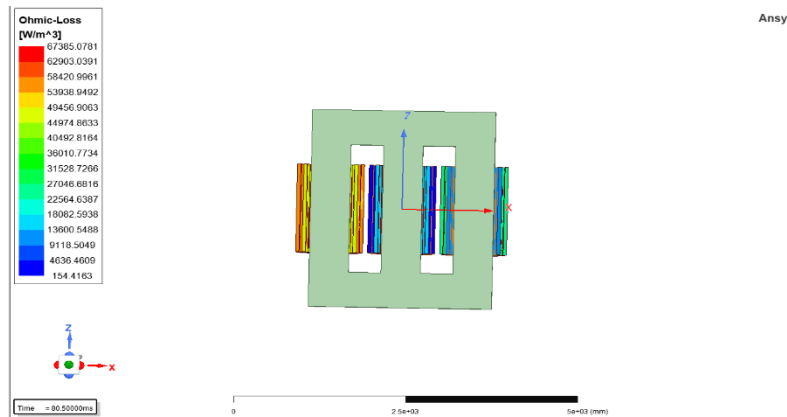


Figure 15: Copper loss

Modeling of the transformer was done with HV winding to analyze the winding loss. Figure 15 shows the winding loss of the transformer in watts/meter cube as $67385\text{W}/\text{m}^3$. The volume of winding was 1.44m^3 . Multiplying them gives a value of 97.03 kW

Table 4: shows a comparison of simulated results with analytical results.

Parameters	Analytical	N_FEM	D_FEM	% Relative Error	% Absolute Error
Core Loss	22.01	19.79	19.62	-12.2	-1.38
Copper loss	104.23	98.47	97.03	-7.4	-1.48

The proposed method outperformed an existing FEM adaptive model, reducing absolute error by 1.48% for copper loss and 1.38% for core loss, and achieving a 12.2% core loss reduction.

Table 5 shows the axial and radial forces across the winding during abnormal operation

Table 5: Abnormal condition

	N_FEM	D_FEM	Analytical
Radial LV Leakage magnetic flux density(T)	-	-	3.9
Radial HV Leakage magnetic flux density(T)	-	-	2.67
Axial LV Leakage magnetic flux density(T)	-	-	3.0
Axial HV Leakage magnetic flux density(T)	-	-	2.04
LV current (A)	11134.04	11134.04	11134.04
HV current (A)	2783.52	2783.52	2783.52
Magnetic flux density	3.61	3.57	3.9

The short circuit current was determined with an asymmetry factor of 1.8, and the leakage flux density in the inner and outer winding of the transformer increased to 3.6 T.

Table 6 shows the axial and radial forces across the winding during abnormal operation

Table 6: Short circuit condition

	Analytical	N_FEM	D_FEM	% Error	Absolute	% Relative Error
Radial LV Force (kN)	1.18	1.27	1.25	-1.60	5.6	
Radial HV Force (kN)	54.61	55.86	54.93	-1.70	0.6	
Axial LV Force (kN)	13.74	13.36	13.51	1.09	-1.7	
Axial HV Force (kN)	634.78	667.03	652.69	-2.20	2.7	

The study conducted a short circuit with an injection of 2783.52A along the primary winding and 11134.04A along the secondary winding, resulting in radial and axial forces computations. The results showed a small absolute error difference of -2.2% and 1.09%, confirming the accuracy of the developed model.

Figure 16 shows the axial force along the low-voltage winding in normal conditions.

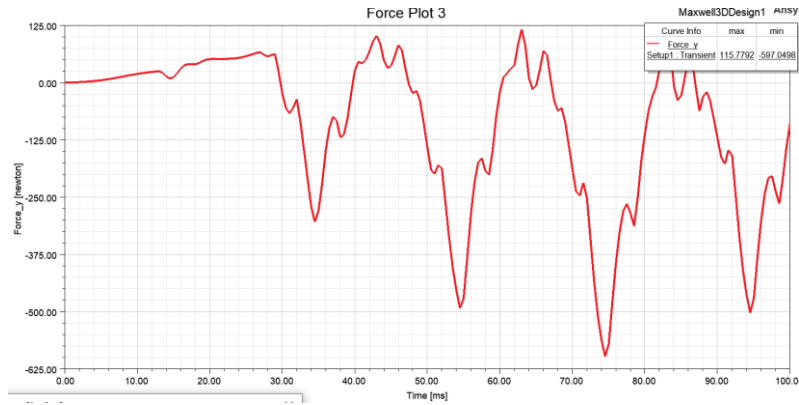


Figure 16: Axial forces at LV on normal condition

It was observed that, during normal conditions, the axial leakage force reaches values of 0.597kN compressing inward.

Figure 17 shows the radial force along the low-voltage winding in normal conditions.



Figure 17: Radial forces at LV on normal condition

It was observed that, during normal conditions, the radial leakage force reaches values of 0.432kN compressing inward.

Figure 18 shows the radial force along the high-voltage winding in an abnormal condition.

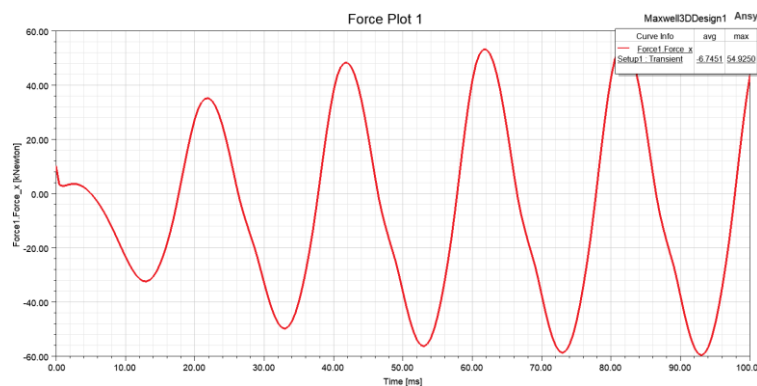


Figure 18: Radial forces at HV on short circuit condition

It was observed that, during normal conditions, the axial leakage force reaches values of 54.93kN compressing inward.

Figure 19 shows the radial force along the low-voltage winding in an abnormal condition.



Figure 19: Radial forces at LV on short circuit condition

It was observed that, during normal conditions, the axial leakage force reaches values of 1.26kN compressing inward.

Figure 20 shows the axial force along the high-voltage winding in an abnormal condition.

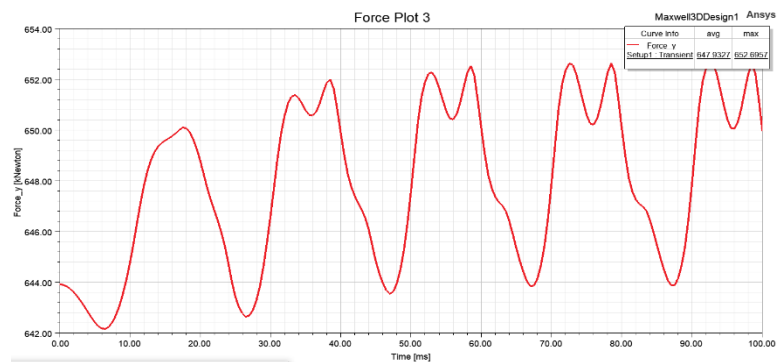


Figure 20: Axial forces at |HV on short circuit condition

It was observed that, during normal conditions, the axial leakage force reaches values of 652.89kN, stressing outward.

Table 7 synthesizes the temperature results at different loading conditions obtained from the thermal model.

Table 7: Temperatures at different loading

Transformer Loading (MVA)	Maximum temperature of the winding
15	86.16°C (ONAN)
30	94.2°C (ONAN)
33	112.9°C (ONAF)

The transformer was tested under overloading conditions, with a 33 MVA load causing no change in core loss but a change in copper loss. The temperature distribution showed a 112.9°C increase on the winding, but an 18°C increase when compared to 30 MVA loading. It was recommended to use the ONAF cooling system for 10% load increments.

Table 8 shows the electrostatic solution across the winding during electrostatic analysis.

Table 8: Electrostatic solution

Electric field (kV/mm)	stress	N_FEM	D_FEM	IEC Standard	% Absolute error
Between HV and LV		10.66	10.48	10-11	-1.72
Between LV and core		3.80	3.74	Less than 2	-1.60
Between HV and dielectric		13.18	13.04	12-17	-1.07

Table 8 compares the D_FEM and N_FEM models during electrostatic analysis, showing a strong correlation with the existing FEM adaptive model. The double discretization model produced smaller stress due to a finer mesh, validating its goal and reducing approximation error to the barest minimum.

Figure 21 shows the electric stresses between LV and HV.

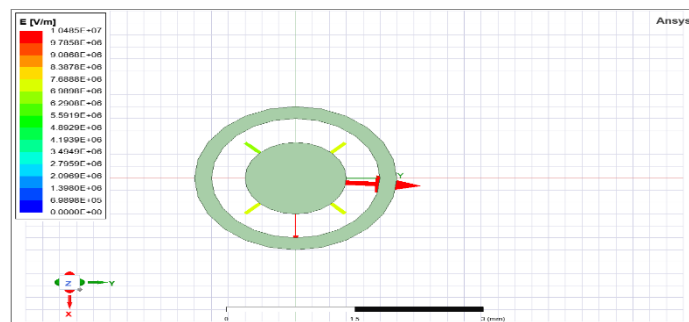


Figure 21: Electric stresses between LV and HV

It was observed that during electrostatic analysis, the electric stress existing between the low and high voltage winding was $10.48\text{kV}/\text{mm}^2$ and is within standard.

Figure 22 shows the electric stresses between the core and the high voltage.

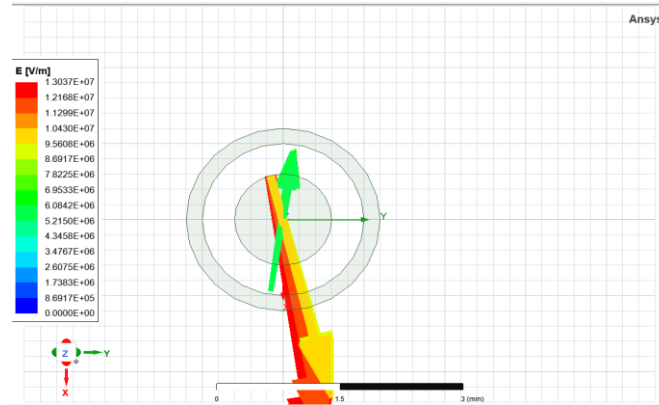


Figure 22: Electrical stresses between HV and Core

It was observed that during electrostatic analysis, the electric stress existing between the core and high voltage winding was $13.04\text{kV}/\text{mm}^2$ and is within standard.

Figure 23 shows the electric stresses between the low voltage and the core.

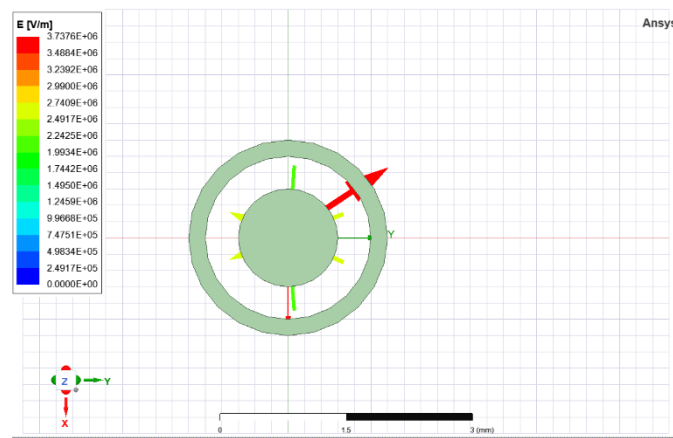


Figure 23: Electrical stresses between LV and Core

It was observed that during electrostatic analysis, the electric stress existing between the core and low-voltage winding was $3.74\text{kV}/\text{mm}^2$ and not within the standard. Then there is a need for an addition of insulation between them to lower the stress.

CONCLUSION

The application of the enhanced Finite Element Method within the ANSYS@MAXWELL environment successfully yielded a high-precision model for analyzing electromagnetic, thermal, and mechanical parameters in power transformer systems. The developed model demonstrated notable accuracy, with reductions in copper and core losses compared to analytical benchmarks, and minimal discrepancies observed in thermal and force analyses. Improvements in electrostatic stress estimation further confirm the robustness of the model. Comparative results between the developed D_FEM and N_FEM approaches highlight a consistent reduction in absolute errors, validating the enhanced method's effectiveness in capturing complex physical behaviors. These outcomes underscore the model's capability for precise and reliable transformer performance assessment, supporting its potential use in optimizing future transformer designs and diagnostics.

REFERENCES

- Abdulkadir, et. al, (2021). 2 kVA, 208/400V, 50 Hz, 3-Phase Transformer Design and Optimization, ResearchGate
- Amir.B., & Dan. F., (2020). Analysis and optimization of a high frequency planar transformer for dc-dc converter using finite element method, Rev. Roum. Sci. Technical ÉlectrotechnicalÉnergy, 2(65), Pp 47-52
- Anionovo U. E., Nwana C. O., Obiora-Okeke C. A., Obute K.C., & Nworabude E. F. (2024). Modeling and Simulation of an Enhanced Finite Element Method for Loss Computation in Power Transformers, UNIZIK Journal of Engineering and Applied Sciences 3(5), Pp1291 – 1306.<https://journals.unizik.edu.ng/index.php/ujeas>
- Behnam H. Ali A. T, & Fatemeh J. (2024), Analysis of Transformer No-Load Loss Using Finite Element Method Validated by Experimental Tests, Research Square, 4(4), <https://doi.org/10.21203/rs.3.rs4296132/v1>
- Bingbing. D., Yu. G., Changsheng. G., Zhu. Z., Tao.W., & Kejie.L., (2021).Three Dimensional Electro Thermal Analysis of a New Type Current Transformer Design for Power Distribution Networks.
- Bolly, R., (2020). Open Circuit and Short Circuit Test on Transformer Phasor Diagram. Circuit, International Journal of Scientific and Technology Research, 3(9), Pp 2277-8616.
- Chitaliya, G., H., & Joshi, S., K., (2021). Finite Element Method for Designing and Analysis of the Transformer, Association of Computer Electronics and Electrical Engineers.
- Cunxiang.Y., Yiwei. D., Hongbo. Q., & Bin. X.,(2021). Analysis of turn-to-turn fault on split winding transformer using coupled field circuit approach.

- Daniel. N., Brydon. S., & Pitshou.B., (2023). Design of an Experimental Approach for Characterization and Performance Analysis of High-Frequency Transformer Core Materials.
- Elzbieta, (2021). Influence of the Selection of the Core Shape and Winding Arrangement on the Accuracy of Current Transformers with Through-Going Primary Cable.
- Elzbieta. L., Michal. K., & Ernest. S., (2020). 3D Electromagnetic Field Analysis Applied to Evaluate the Accuracy of a Voltage Transformer under Distorted Voltage.
- Fausto.V., Hugo.A., & Franklin Q., (2021).Prediction of Stress in Power Transformer Winding.
- Hernandez. C., Jorge. L., Marco. A., & Enrique. V., (2023) Multiobjective Electromagnetic Design Optimization of a Power Transformer using 3D Finite element analysis, response surface methodology, and the third Generation non-sorting Genetic Algorithm. <http://dx.doi.org/10.5755/j02.eic.29238>
- Ji.H. L., Hoon. K. L., Young. G. L. Jeong.I. L., Seong.T. J., Kyong. H., Kim J.Y. P., & Jang.Y. C., (2022). Design and Analysis Considering Magnet Usage of Permanent Magnet Synchronous Generator Using Analytical Method
- Kamran. D., Fatih. I., & Guven. K.,(2022). Comparison of analytical method and different finite element methods for calculation of leakage inductance in zigzag transformers, *ElektronikaIr Elektrotehnika*,1(28).
- Liu, D., Wei, B., Cai, C., Ding, J., & Guo, Z.,(2020) TOC Optimization Design of Amorphous Metal Core Distribution Transformer Based on NSGA-II. In *Proceedings of the 2020 IEEE International Conference on Applied Superconductivity and Electromagnetic Devices (ASEMD)*,1(8), Pp. 1-2.
- Nivashini. L. M., Madhumitha. K.,&Sindhus. S., (2020). Design of high voltage transformer using finite element method, *International journal of scientific and technology research*, 3(9).
- Orosz, T.,Pánek, D.,Karban, P.,(2020) FEM Based Preliminary Design Optimization in Case of Large Power Transformers. *Appl. Sci*,1(10), Pp3-6.
- Pei. H., Renjun. D., Peng. W., Dan. W., Zhenxing.L., & Qi. W., (2021) Comprehensive Analysis of Electric Field Characteristics for Multi Winding Medium Frequency Transformer
- Piotr.O., & Pawel. W.,(2023) Analyses the Core Losses in Transformer working tt Static Var Compensator Powertech Transformers, Tel 012 318-9911
- Samuel B., Van N. L., & Henri C.,(2021) A Nonlinear Finite Element Analysis Tool to Prevent Rupture of Power Transformer Tank.
- Sheoran.K., Dash.P., & Kumar. V.,(2020). Modeling and Analyzing Electromagnetic Short Circuit Forces In Single And Double Helical Windings Of Transformer Using Finite Element Method, *International Journal of Recent Trends in Engineering and Research (IJRTER)*, 6(6)
- Syed, M. H., Rohit, S., Manas, R. M., & Sattam, S. A., (2020). Hydro magnetic Dissipative and Radioactive Grapheme Maxwell Nano fluid Flow Past a Stretched Sheet Numerical and Statistical Analysis.
- Tan, Y., Yu, X., Wang, X., L.V, Q, & Shi, M.,(2022) Interaction Analysis and Multi Response Optimization of Transformer Winding Design Parameters. *International.Communication.Heat Mass Transfer*, 13(7).